The Journal of Immunology

Lasting Antibody Responses Are Mediated by a Combination of Newly Formed and Established Bone Marrow Plasma Cells Drawn from Clonally Distinct Precursors

Irene Chernova, Derek D. Jones, Joel R. Wilmore, Alexandra Bortnick, Mesut Yucel, Uri Hershberg and David Allman

J Immunol 2014; 193:4971-4979; Prepublished online 17 October 2014;
doi: 10.4049/jimmunol.1401264
http://www.jimmunol.org/content/193/10/4971

The Journal of Immunology is published twice each month by
The American Association of Immunologists, Inc.,
9650 Rockville Pike, Bethesda, MD 20814-3994.

Print ISSN: 0022-1767 Online ISSN: 1550-6606.

Lasting Antibody Responses Are Mediated by a Combination of Newly Formed and Established Bone Marrow Plasma Cells Drawn from Clonally Distinct Precursors

Irene Chernova,* Derek D. Jones,* Joel R. Wilmore,* Alexandra Bortnick,* Mesut Yucel,† Uri Hershberg,‡ and David Allman*

Current models hold that serum Ab titers are maintained chiefly by long-lived bone marrow (BM) plasma cells (PCs). In this study, we characterize the role of subpopulations of BM PCs in long-term humoral responses to T cell–dependent Ag. Surprisingly, our results indicate that 40–50% of BM PCs are recently formed cells, defined, in part, by rapid steady-state turnover kinetics and secretion of low-affinity IgM Abs. Further, for months after immunization with a hapten–protein conjugate, newly formed Ag-induced, IgM-secreting BM PCs were detected in parallel with longer-lived IgG-secreting cells, suggesting ongoing and parallel input to the BM PC pool from two distinct pools of activated B cells. Consistent with this interpretation, IgM and IgG Abs secreted by cells within distinct PC subsets exhibited distinct L chain usage. We conclude that long-term Ab responses are maintained by a dynamic BM PC pool composed of both recently formed and long-lived PCs drawn from clonally disparate precursors. ***The Journal of Immunology*****, 2014, 193: 4971–4979.**

Conventional wisdom holds that lasting serum Ab titers reflect the activity of long-lived plasma cells (PCs) localized in specialized niches in the bone marrow (BM) (1). It is generally assumed that most BM PCs are long-lived and derived from germinal centers (GCs), specialized microenvironments enriched for Ag-stimulated B cells undergoing class switch recombination, somatic hypermutation, and affinity-driven selection (2). However, BM PCs also arise via GC-independent pathways (3–6), and many memory B cells also arise without maturing in GCs (7, 8). However, the extent to which the GC-driven and GC-independent pathways contribute to long-lived BM PC pools is unknown.

Newly formed PCs are thought to enter the BM as immature cells where they must compete for limited survival niches in the BM (1). This possibility is consistent with three reports describing immature plasmablast-like PCs in the BM (5, 9, 10). Furthermore, it has been proposed that newly formed PCs must supplant previously generated PCs to achieve longevity (11). However, to our knowledge, a comprehensive study of the cellular dynamics of the BM PC pool together with an assessment of the kinetics and duration with which recently induced PCs enter and persist in the BM has not been performed.

Our work examines the cellular dynamics of distinct BM PC populations and their role in long-lived humoral immunity. Surprisingly, at steady-state, >40% of Ab-secreting BM PCs share multiple features with immature PCs in the spleen or lymph nodes, because these cells express the B cell surface Ags B220 and CD19, exhibit a rapid 50% renewal rate of 2–3 d, and possess relatively low concentrations of the PC-requisite transcription factor Blimp-1 (10). These results indicate that a considerable fraction of the BM PC pool relies on routine input from peripheral tissues. Equally surprising, on immunization of C57BL/6 (B6) adults with the hapten–protein conjugate nitrophenyl-chicken γ–globulin (NP-CγG), some 50% of NP-specific PCs were detected within the immature BM PC subset for months postimmunization, suggesting that Ag depots drive the generation of new PCs long after immunization. Furthermore, although NP-specific responses in B6 mice are dominated by a single clone defined, in part, by utilization of λ1 Ig L chains, nearly all cells within the newly formed $B220^+$ fraction of BM PCs secreted $IgM^+\kappa^+$ Abs. These results suggest that IgM^+ memory cells produce PCs continuously throughout much of the primary immune response. Altogether, these results indicate that lasting Ab responses are mediated by the combined activity of immature and mature BM PCs derived from clonally distinct pools of activated B cells.

Materials and Methods

Mice

C57BL/6 (B6) females (age 8–10 wk) were obtained from Jackson Laboratories and housed in our colony for at least 2 wk before analysis. B6.$Blimp1^{+/GFP}$ mice (10) were kindly provided by Dr. Mark Pescovitz (Indiana University, Bloomington, IN) with permission from Dr. Stephen Nutt (Walter and Eliza Hall Institute of Medical Research, Parkville, VIC, Australia). All animal procedures were approved by the University of Pennsylvania Office of Regulatory Affairs.

Flow cytometry and cell sorting

Spleen and BM cells were harvested and stained with the indicated Abs as described previously (12). Unless noted otherwise, all reagents were purchased from eBioscience: FITC–anti-IgM (R26-46; BD Pharmingen) and PNA (Sigma-Aldrich); PE–anti-CD138 (281-2; BD Pharmingen); PE–Texas

*Department of Pathology and Laboratory Medicine, University of Pennsylvania School of Medicine, Philadelphia, PA 19104; †Department of Bioengineering, Ege University, 35100, Izmir, Turkey; and ‡School of Biomedical Engineering Science and Health Systems, Drexel University, Philadelphia, PA 19104

Received for publication May 19, 2014. Accepted for publication September 13, 2014.

This work was supported by National Institutes of Health Grants RO1AI097590 (to D.A.), F30HL112628 (to I.C.), T32CA009140 (to D.D.J.), and T32 AI070099 (to A.B.).

Address correspondence and reprint requests to Dr. David Allman, University of Pennsylvania, 36th Street and Hamilton Walk, 230 John Morgan Building, Philadelphia, PA 19104-6082. E-mail address: dallman@mail.med.upenn.edu

The online version of this article contains supplemental material.

Abbreviations used in this article: BM, bone marrow; GC, germinal center; NP, nitrophenyl; NP-CγG, nitrophenyl-chicken γ–globulin; PC, plasma cell.

www.jimmunol.org/cgi/doi/10.4049/jimmunol.1401264

Red–anti-B220 (RA3-6B2); PE–Cy7–anti-CD4 (RM4-5), anti-CD8α (53-6.7), anti–Gr-1 (RB6- 8C5), anti-F4/80 (BM8), and anti-TER119; allophycocyanin–Cy5.5–anti-CD19 (1D3); Alexa405 anti-IgD (11–26), and Biotin–anti-CD138 (281-2; BD Pharmingen). Biotinylated Abs were revealed with streptavidin- allophycocyanin-Cy7 (BD Pharmingen). Allophycocyanin-NP was conjugated in our laboratory. Nonviable cells were eliminated from analyses with the UV-excited DNA dye DAPI (Molecular Probes), and doublets were excluded based on the width of the forward and side scatter signals. For intracellular stains, live cells were identified by preincubation with AquaLIVE/DEAD fixable live/dead stain (Invitrogen). Cells were fixed and permeabilized using solutions A and B (Caltag). For PC and B cell subset labeling in vivo, B6.Blimp1$^{+/GFP}$ adults were given a single i.v. injection of 0.4 μg PE–anti-CD138 or PE–anti-CD19, then sacrificed 2 min later. Resulting cell preps were then subjected to standard cell-surface staining protocols. Flow cytometry was performed on a BD LSRII, and cell sorting was performed on a four-laser Aria (Becton Dickinson). Analysis was done using FlowJo8.8 (Tree Star).

In vivo BrdU labeling

Adult B6 mice were fed drinking water containing 0.5 mg/ml BrdU and 1 mg/ml sucrose. Flow-cytometric analysis of BrdU incorporation was accomplished as previously described (12) using FITC–anti-BrdU Abs (Becton Dickinson).

Computational modeling

The maximum number of actively dividing PCs based on BrdU pulse-chase labeling data were estimated with the following equations.

For the increasing parts of the curve:

$$\frac{dU}{dt} = -(p+d)U$$

$$\frac{dL}{dt} = pU + (p-d)L$$

And for the decreasing parts of the curve:

$$\frac{dU}{dt} = (p-d)U + pL$$

$$\frac{dL}{dt} = -(p+d)L$$

Where U and L indicate unlabeled and labeled cell numbers, respectively, and p and d represent proliferation and death rates (1/time). These formulas can be converted into the following fractions:

$$U_{f(t)} = \frac{U_{(t)}}{U_{(t)} + L_{(t)}}, L_{f(t)} = \frac{L_{(t)}}{U_{(t)} + L_{(t)}}$$

Because there are only two components, $U_{f(t)} + L_{f(t)} = 1$. Results from these calculations for the increasing part of the curve are shown in Supplemental Table 1.

Immunizations

Eight- to twelve-wk-old mice were immunized i.p. with 50 μg NP_{16}-CGG in alum. Multiscreen HTS plates (Millipore) were coated with 10 μg/well of either goat anti-mouse Ig(H+L) (Southern Biotech), or NP_{33}-BSA, or NP_4-BSA (BioSearch) in sodium bicarbonate buffer.

ELISPOT and ELISA analyses

For ELISPOTs, cells were serially diluted across the plate and then incubated for 4–8 h at 37°C. Biotin–goat anti-IgG, goat anti-IgM, or goat anti-IgG1 (Southern Biotech) diluted in block buffer was added, followed by three washes with 0.1% Tween 20 detergent, and a secondary incubation with ExtrAvidin-alkaline phosphatase (Sigma-Aldrich). Spots were detected using BCIP/NBT (Sigma-Aldrich), and scanned and counted with an ImmunoSpot Analyzer (Cellular Technology). To assess frequencies of hapten-specific PCs within defined subsets, 2–20 × 10^3 B220$^+$ CD138^{high} or B220$^-$ CD138^{high} BM cells were sorted into ELISPOT plates, and the fraction of these cells secreting NP-specific Abs was determined as described earlier. This number was multiplied by the overall frequency of cells within the relevant subpopulation as a function of all BM cells followed by the total number of BM cells as determined by Opstelten and Osmond (13). For ELISAs, 2-fold dilutions of sera from immunized or control animals were added to NP_{26}-BSA–coated 96-well plates and processed via standard procedures. Plates were developed with HRP-conjugated H or L chain isotype-specific Abs at optimal dilutions. After subtracting average background readings, titers were calculated as the greatest dilution to achieve an OD of 0.1.

Cell morphology

A total of 10^4 sorted cells were centrifuged onto microscope slides (800 rpm, 3min) with a Cytospin, fixed in ethanol (95% EtOH for 10 min, 70% EtOH for 30 s), and stained with eosin for 3 min followed by hematoxylin for 1 min. Images were obtained on a Nikon Eclipse TE2000-U microscope and captured using a Nikon DA-Fi2 camera.

Statistical analysis

Significances in differences in PC frequencies between two experimental groups were evaluated with the unpaired two-tailed t test using Excel software.

Results

Resolution of three BM PC subsets

We noted recently that many NP-specific PCs in the BM of NP-LPS–immunized mice retain expression of the naive B cell surface protein B220 (3). Because B220 and CD19 expression are thought to be downregulated during early phases of PC differentiation (14), this observation, together with other recent reports of BM PCs with properties of immature Ab-secreting cells (5), led us to evaluate B220 and CD19 surface expression on all BM PCs. To identify rare BM PCs effectively, we first focused on cells coexpressing the PC-associated surface protein CD138 (15) and Blimp-1 in adult B6.Blimp1$^{+/GFP}$ reporter knock-in mice that were not immunized intentionally (10). Because some T cells are Blimp1^{low} (16, 17), we intentionally excluded TcRβ$^+$ cells from these analyses. As shown, in B6.Blimp1$^{+/GFP}$ adults, some 60% of BM PCs (TcRβ$^-$ Blimp1/GFP$^+$ CD138^{high}) coexpressed B220 and CD19 (Fig. 1A), and surface CD19 expression was also readily evident among approximately two thirds of the remaining B220$^-$ Blimp1/GFP$^+$ CD138^{high} cells. We also resolved three populations of CD138^{high} BM cells in conventional B6 adults defined by differential B220 and CD19 surface expression (Fig. 1B). These included B220$^+$ CD138^{high} cells (gate b) that were also CD19$^+$ (corresponding to the B220$^+$ CD19$^+$ population illustrated in Fig. 1A) and B220$^-$ CD138^{high} cells that consisted of both CD19$^+$ (gate c) and a minor CD19$^-$ population (gate d) corresponding to the B220$^-$ CD19$^+$ and B220$^-$ CD19$^-$ subsets in Fig. 1A. Notably, although the levels of surface B220 expression on the BM PC populations defined in this article are somewhat lower than typically observed on mature B cells and encompass a broad range in surface protein expression, for simplicity, in this article, we refer to these PC subsets as B220$^+$ and B220$^-$.

Based on ELISPOT analyses with cells sorted from B6 adults, all three CD138^{high} subpopulations were highly enriched for cells characterized by active Ab secretion (Fig. 1C). These cells are clearly distinct from a previously described B220^{low} CD138^{low} pre-B cell fraction found in gate a in Fig. 1B (18), because this population lacked cells secreting Ab and Blimp-1 expression (Fig. 1C, 1F). We should also note that B220$^+$ CD138^{high} BM PCs do not appear to correspond to the pre-PCs described in Ig transgenic mice, because pre-PCs do not actively secrete Abs (19). As expected, when derived from B6 adults, cells within these subpopulations exhibited substantial *Prdm1* (Blimp1) transcript abundance, although Prdm1 transcripts were lower for B220$^+$ CD138^{high} cells. These populations also exhibited minimal transcript levels for the B-lineage master transcription factor Pax5, which is downregulated upon induced PC differentiation (Fig. 1D) (14). Cells within the CD138^{high} B220$^+$ and CD138^{high} B220$^-$ fractions also exhibited cell morphology consistent with full PC differentiation (Fig. 1E). Finally, when we applied the

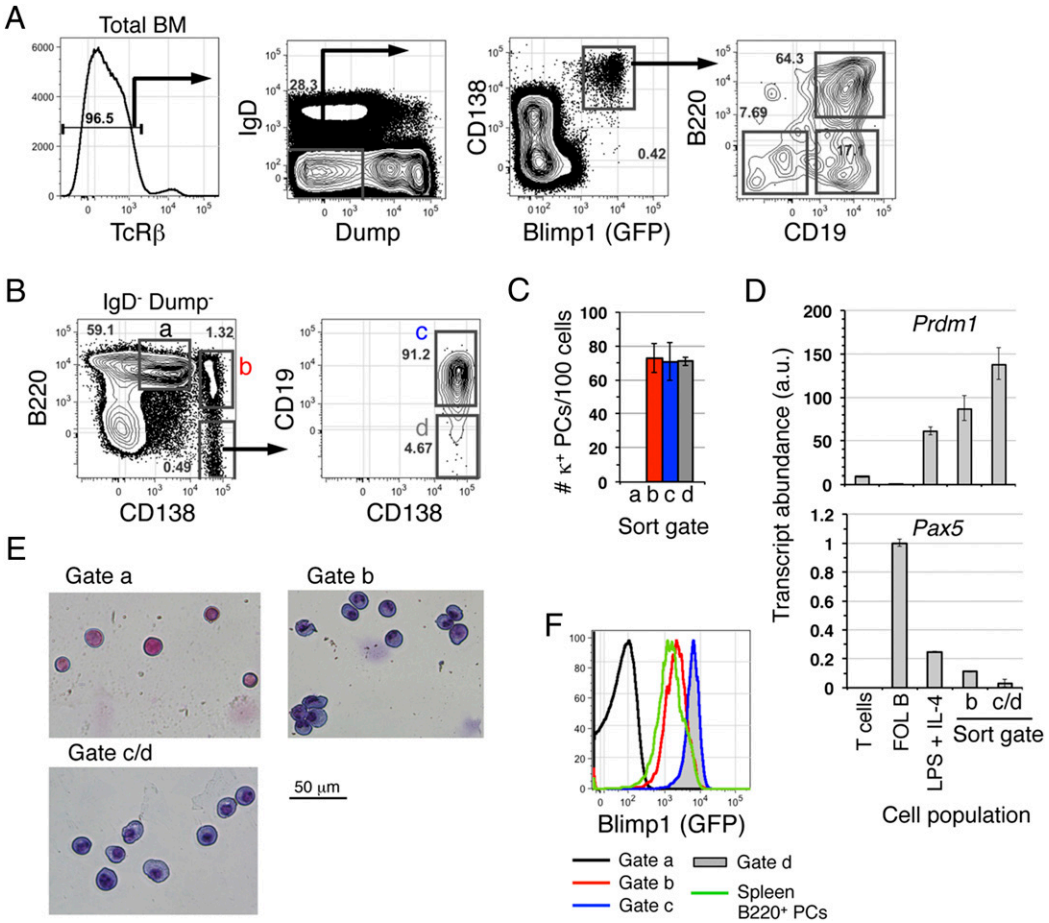

FIGURE 1. Resolution of three populations of BM PCs. (**A**) BM cells from an 8-wk-old female B6.Blimp1$^{+/GFP}$ mouse were stained with the indicated Abs before analysis of 2×10^6 events. The *leftmost* plot is pregated on DAPI$^-$ cells. Arrows indicate each successive gate. "Dump" Abs were F4/80, Gr-1, Ter-119, CD4, and CD8α. Representative of four separate analyses. (**B**) BM cells from an 8-wk-old female B6 mouse were stained and analyzed as in (A). Representative of 10 separate analyses. (**C**) Cells from the indicated populations were sorted and added in triplicate to ELISPOT plates coated with anti-mouse Igκ and Igλ Abs. Representative of two separate experiments. (**D**) cDNA prepared from CD3$^+$ T cells, splenic CD23$^+$ follicular (FOL) B cells, FOL B cells stimulated with LPS + IL-4 for 3 d, or cells within the indicated BM PC subsets (B) were sorted from adult B6 mice and subjected to RT-PCR using TaqMan probes for Blimp1 (Prdm1), Pax5, or GAPDH. Resulting signals were normalized to FOL B cells. (**E**) Cells were sorted from adult B6 mice using the gates shown in (B) and stained with H&E as described in *Materials and Methods*. (**F**) BM or spleen cells from an 8-wk-old female B6.Blimp1$^{+/GFP}$ mouse were stained as in (B), and relative GFP expression was determined using the gating strategies shown in (B) and summarized in Fig. 2.

gating strategy illustrated in Fig. 1B to BM cells derived from a B6.Blimp1$^{+/GFP}$ adult, it was clear that cells in all three BM CD138^{high} subpopulations exhibit substantial levels of Blimp1 expression (Fig. 1F), although it should be noted that cells within the CD138^{high} B220$^+$ BM fraction possessed significantly lower Blimp1/GFP levels compared with their B220$^-$ counterparts in the BM, yet similar levels to immature splenic B220$^+$ PCs. Together, these data indicate that BM PCs can be subdivided into at least three subsets based on differential B220 and CD19 surface expression. Furthermore, data revealing relatively low Blimp1 expression for B220$^+$ CD138^{high} BM cells suggest that these cells are the least mature PCs within the BM PC pool (10).

The majority of B220$^+$ BM PCs are recently formed

Past work has shown that immature splenic PCs label with rapid and linear kinetics, achieving near 100% labeling within 3 d (20). Accordingly, we defined steady-state cellular renewal rates for each BM PC subpopulation using continuous in vivo BrdU labeling. We gave cohorts of B6 adults BrdU for up to 60 d and determined the proportion of BrdU$^+$ cells for the total BM PC pool, as well as for each BM PC subset at multiple time points. Small, nondividing pre-B cells (FSC^{low} B220^{low} CD43$^-$ IgM$^-$), which exhibit near-complete cellular turnover every 3 d (21), were used to control for the efficiency of BrdU labeling. As shown (Fig. 2A), some 30% of the total BM PC pool became BrdU$^+$ within 5 d, and within 25 d just >40% were BrdU$^+$. As expected, within 3 d, small pre-B cells were nearly 100% BrdU$^+$. Most notably, when subdivided based on B220 surface expression, B220$^+$ PCs in the BM exhibited markedly rapid labeling kinetics, achieving 80% labeling within 5–6 d with a 50% renewal rate of 2–2.5 d (Fig. 2B). These labeling kinetics are comparable with extrafollicular splenic PCs (22). In contrast, labeling rates for B220$^-$ BM PCs were relatively protracted, reaching 35% BrdU$^+$ by day 25, then plateauing at later time points. Labeling kinetics for B220$^-$ CD19$^+$ and B220$^-$ CD19$^-$ PCs were indistinguishable from one another.

To examine the turnover kinetics and potential precursor–successor relationships for these BM PC subsets more closely, we performed pulse-chase experiments in which mice were fed BrdU for 6 d, with percent labeling assessed at several time points before and after terminating BrdU labeling. As shown (Fig. 2C), during the chase period, the fraction of BrdU$^+$ cells within the B220$^+$ BM PC fraction dropped from 80% to <20% within 4 d, reaching background levels by day 6. Surprisingly, although B220$^+$ PCs comprise some 50% of the BM PC pool and were 80%

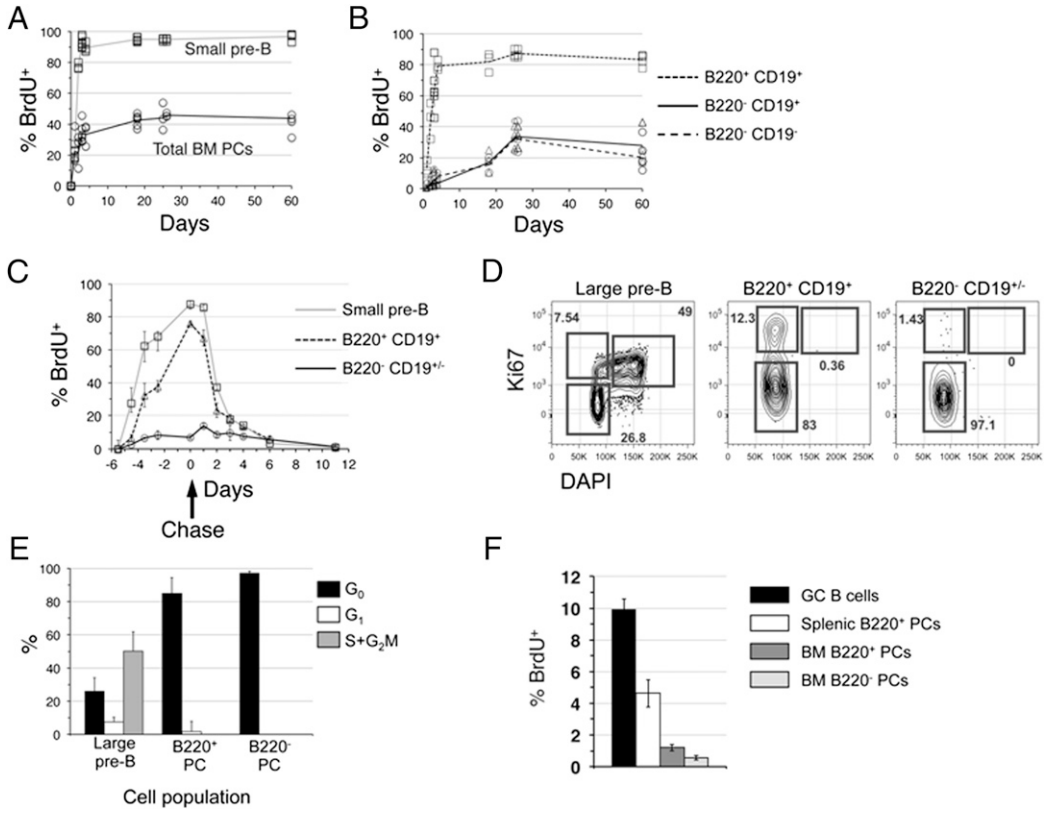

FIGURE 2. Many BM PCs are recently formed. (**A**) B6 mice were fed BrdU for the indicated days before determination of the percent $BrdU^+$ cells among all $Dump^-$ IgD^- $CD138^{high}$ BM cells. Small pre-B cells were gated as FSC^{low} $B220^{low}$ $AA4^+$ IgM^- cells. Best-trend lines were drawn across the mean percent $BrdU^+$ cells for each population using three to four mice per time point. (**B**) The flow cytometric data in (A) were gated as shown in Fig. 1B to determine the fraction of $BrdU^+$ cells in the indicated populations at each time point. (**C**) B6 adults were given BrdU for up to 6 d and then given BrdU-free drinking water (chase) for another 12 d. The fraction of $BrdU^+$ cells in each BM population was determined as in (A) and (B). (**D**) BM cells from 12-wk-old B6 mice were stained to resolve large pre-B cells (FSC^{high} $B220^{low}$ $AA4^+$ IgM^-) or PC subsets based on differential B220 expression, fixed and permeabilized, and then stained with anti-Ki67 Abs and DAPI. (**E**) Data summarized for three mice using gates shown in (D). Representative of two separate experiments. (**F**) Eight-week-old B6 mice were inoculated with BrdU. Sixty minutes later, $BrdU^+$ cells were identified among the indicated BM and spleen cell populations. GC B cells were identified as $CD19^+$ IgD^- $CD38^-$ PNA^{high} cells.

$BrdU^+$ on day 6, we detected few, if any, $BrdU^+$ cells within the $B220^-$ fraction during either the labeling or the chase periods. These data suggest that, at steady-state, relatively few $B220^+$ BM PCs create longer-lived $B220^-$ PCs.

Because early PC populations may include dividing cells (23), we used two separate strategies to assess proliferation among $B220^+$ and $B220^-$ BM PCs. First, we measured the DNA content of cells within each subset with the DNA dye DAPI together with Ki67 Abs. Recent work has shown that this combined approach allows resolution of cells in the G_0 ($Ki67^-$, 2N), G_1 ($Ki67^+$, 2N), and S + G_2/M ($Ki67^+$, >2N) phases of the cell cycle (24). We were unable to detect cells in the S or G_2/M phase within any BM PC population (Fig. 2D, 2E), although cell division was readily apparent in large pre-B cells (FSC^{high} $B220^{low}$ $CD43^-$ IgM^-) (25). Because exposure to BrdU can induce division of BM progenitors (24), we also performed these analyses with mice given BrdU for 6 d; however, exposure to BrdU did not alter Ki67 or DNA content profiles for any BM PC subpopulation (data not shown). Second, we used a 60-min in vivo BrdU pulse strategy shown to label dividing B-lineage cells selectively and efficiently (26). Whereas this approach led to the identification of proliferative GC B cells and a small fraction of $BrdU^+$ PCs in the spleen, we were unable to detect $BrdU^+$ $B220^+$ PCs in the BM with this approach (Fig. 2F and Supplemental Fig. 1). Together, these data suggest that $B220^+$ BM PCs are largely nonproliferative cells derived from proliferative precursors.

To evaluate the role of cell division in the homeostasis of BM PC populations more closely, we used mathematical modeling algorithms formulated to determine the minimal degree of cell division required to explain the BrdU labeling kinetics observed for $B220^+$ BM PCs (see Supplemental Table I) (27). When we fit the on or off labeling segments of the BrdU pulse-chase data in Fig. 2C to a simple single-compartment proliferation model (see *Materials and Methods*), we find that for the observed BrdU labeling kinetics to reflect active cell division, 16–30% of $B220^+$ BM PCs would need to undergo cell division every day. Because the observed fraction of actively dividing cells is far less, we conclude that most newly formed BM PCs are nondividing cells derived from actively dividing precursors, as described previously for memory B cells (27). When considered together, the BrdU labeling and cell-cycle analysis data allow two conclusions. First, we conclude that 40–50% of BM PCs are replaced by incoming cells every 5–6 d. Second, given the nonlinear nature of the labeling kinetics obtained for $B220^-$ BM PCs (Fig. 2B), we suggest that this PC fraction contains at least two subpopulations characterized by intermediate versus lengthy life spans.

Immature BM PCs are not enriched in marrow sinusoids

One possibility is that $B220^+$ PCs harvested from BM cell preparations are localized in sinusoids in situ, allowing for ready recirculation throughout the vasculature. Alternatively, $B220^+$ BM PCs

may be positioned within bona fide PC niches in the BM parenchyma. To distinguish these possibilities, we adopted an in vivo Ab labeling approach used previously to identify B-lineage progenitors localized to sinusoids versus the BM parenchyma (28). With this strategy, cells localized within sinusoids become labeled only 2 min after i.v. injection of PE-labeled Abs specific for relevant cell-surface proteins, whereas within this time frame cells within the BM parenchyma remain unlabeled. We inoculated B6.Blimp1$^{+/GFP}$ adults with PE–anti-CD138 or PE–anti-CD19 Abs, then 2 min later assessed PE labeling among B220^{+} and B220^{-} Blimp1/GFP^{+} cells in the spleen and BM, and pre-B and immature B cells in the BM. As shown (Fig. 3A, 3C), whereas a large fraction of splenic PCs became labeled with this approach, cells within the B220^{+} and B220^{-} BM PC fractions remained unlabeled. By contrast, consistent with the notion that a considerable fraction of CD19^{+} immature B cells are found in BM sinusoids (28), immature BM B cells were readily labeled upon i.v. inoculation with anti-CD19 Abs, but pro- and pre-B cells, known to be localized within the BM parenchyma, were not (Fig. 3B, 3C). We conclude that B220^{+} BM PCs are not found within BM sinusoids.

Role of B220^{+} BM PCs in long-term responses

Next, we probed the roles played by B220^{+} and B220^{-} BM PCs in induced T cell–dependent Ab responses. To establish the kinetics with which PCs enter and persist within each population, we quantified NP-specific PCs among sorted B220^{+} and B220^{-} BM PCs at several time points between 6 and 130 d after a single inoculation with NP-CγG (Fig. 4A). Remarkably, we detected hapten-specific cells in both pools at all time points examined, even out to day 130, although after 100 d somewhat fewer NP-specific PCs localized to the B220^{+} BM fraction (Fig. 4A). When considered in tandem with the BrdU labeling data in Fig. 2, these data suggest that recently formed Ab-secreting cells continue to seed the BM PC pool long after a single immunization. To test this idea further, we immunized additional mice with NP-CγG, and 30 d later added BrdU to their drinking water for an additional 7 d before assaying for BrdU^{+} NP-binding BM PCs. As shown (Fig. 4B), some 9% of all detectable NP-binding BM PCs were BrdU^{+}, and as expected, these cells were B220^{+}. We conclude that newly formed PCs contribute to the BM PC pool well after initiation of T cell–dependent humoral responses.

Past studies indicate that Ag-activated or Ag-experienced B cell populations can be identified in peripheral tissues long after exposure to Ag and without maturing in GCs. For instance, Hsu et al. (29) detected extrafollicular plasmablasts for extended periods in the spleens of mice immunized once with the type 2 T cell independent Ag NP-Ficoll, and recent findings indicate that many memory B cells are GC-independent IgM^{+} cells (7, 8), and hence consist mainly of cells bearing relatively low-affinity Ag receptors. Therefore, we considered the possibility that some BM PCs that form late in the NP-CγG response might not secrete high-affinity class-switched Abs. Accordingly, we examined the H chain isotype of Abs secreted by B220^{+} and B220^{-} BM PCs at multiple time points ranging from 27–134 d postimmunization with NP-CγG. To measure PCs secreting high-affinity class-switched Abs, we used ELISPOT plates coated with proteins with a low NP-carrier molar ratio (30). Strikingly, whereas the B220^{-} fraction contained cells secreting either IgM or high-affinity IgG Abs, within the B220^{+} fraction, hapten-specific PCs were composed almost exclusively of IgM-secreting cells (Fig. 5A, 5B). These results indicate that B220^{+} and B220^{-} BM PCs play functionally distinct roles in maintaining Ab titers in response to NP-CγG, while further suggesting that Ab-secreting cells in each pool arise from clonally unrelated precursors. To probe the latter notion further, we performed additional experiments to characterize Ig L chain usage by NP-specific PCs in each population, again at several time points postimmunization. As shown in Fig. 5C, whereas hapten-specific PCs within the B220^{-} BM PC fraction secrete Abs using either Igκ or Igλ L chains, beginning 50 d postimmunization, NP-specific Abs secreted by B220^{+} BM PCs were almost exclusively Igκ^{+}. The failure to detect Igλ^{+} PCs among the B220^{+} BM fraction at later time points may be because of the failure of GCs induced by NP-CγG immunization to persist for extended periods (31), but may also reflect an exceptionally long life span for IgM^{+} memory B cells suggested by several recent studies (8, 31, 32). Finally, as expected, early postimmunization NP-specific serum Abs were mainly Igλ^{+}. However, consistent with our ELISPOT data, by 50 d postimmunization, a considerable fraction of NP-specific serum Abs were Igκ^{+} (Fig. 6).

Candidate memory B cell populations

The predominance of cells secreting IgMκ^{+} Abs in the NP-specific B220^{+} BM fraction led us to examine L chain usage among peripheral NP-specific IgM^{+} memory cells using criteria for memory B cells established by Shlomchik and colleagues (33). Although

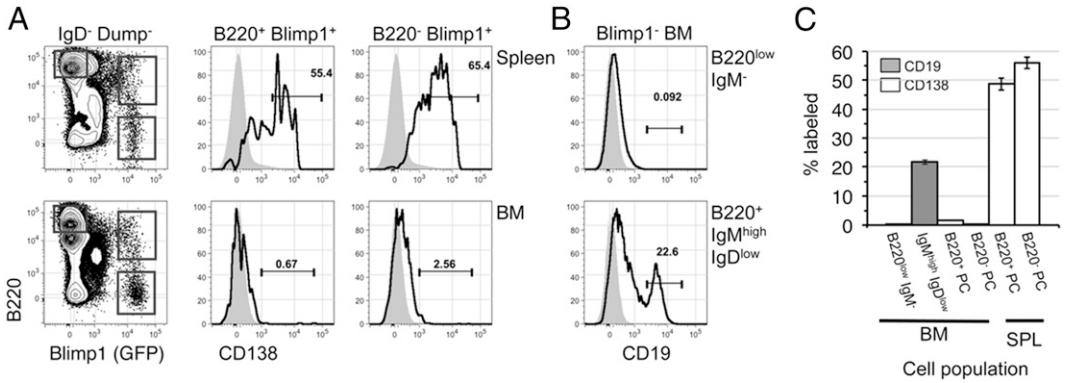

FIGURE 3. B220^{+} marrow PCs are not located in BM sinusoids. (**A** and **B**) B6.Blimp1$^{+/GFP}$ adults were given a single i.v. inoculation of 0.4 μg PE-CD138 or PE-CD19. Two minutes later, mice were sacrificed and BM and spleen cells stained with the indicated Abs (excluding CD138 and CD19) before flow cytometric analysis of 2.5 × 10^{6} events. (A) Representative CD138 labeling of spleen (*top panel*) or BM (*bottom panel*) cells is shown. *Leftmost* plots are pregated on viable Dump^{-} IgD^{-} cells as in Fig. 1. Overlay histograms illustrate CD138 signal on the indicated PC subsets (black line), with the indicated B220^{high} Blimp1/GFP^{-} gates used to establish background signal (gray filled). (B) CD19 labeling for BM pro-/pre-B cells (GFP^{-} B220^{low} IgM^{-}) and immature (GFP^{-} B220^{+} IgM^{high} IgD^{low}) B cells. Gray filled curves are from mice that were not inoculated with PE-labeled Abs. (**C**) Mean and SEM of percent labeled cells within the indicated populations, with three to five mice per group summarized from two separate experiments.

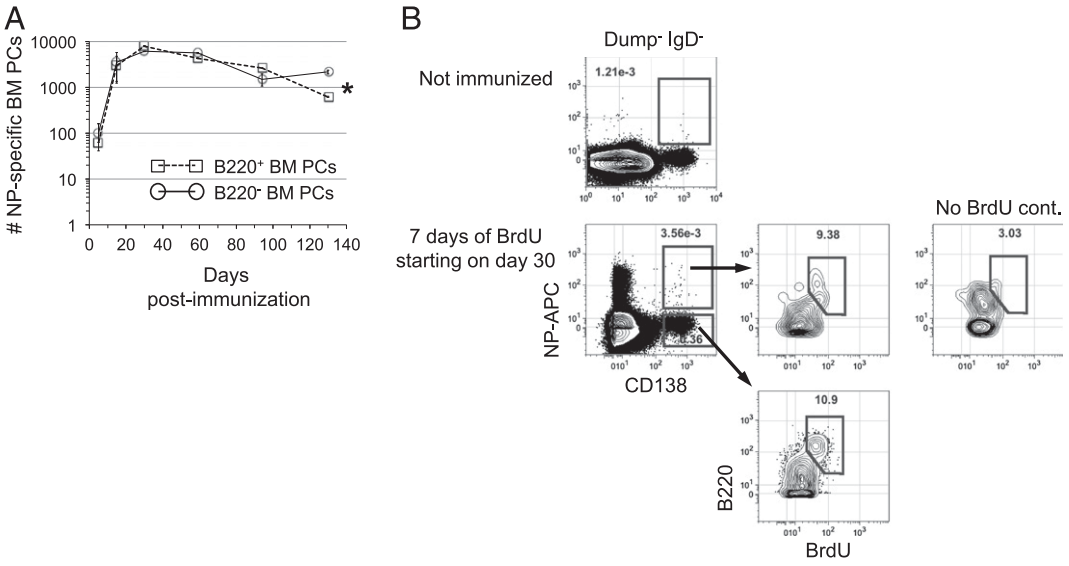

FIGURE 4. Ag-induced PCs colonize the B220$^+$ BM PC subset for months postimmunization. (**A**) Adult B6 mice were immunized with NP-CγG, and at the indicated time points, B220$^+$ and B220$^-$ BM PCs were sorted into NP_{26}-BSA–coated ELISPOT plates that were subsequently probed with anti-Igκ and anti-Igλ Abs. Numbers of hapten-specific PCs in the BM at each time point were calculated as described in *Materials and Methods*. Error bars represent SEM of triplicate ELISPOT wells. Background has been subtracted out. *$p < 0.05$. (**B**) B6 mice were immunized with NP-CγG. At day 30 postimmunization, mice were fed BrdU (or not) for an additional 7 d, and BM CD138^{high} B220$^{+/-}$ PCs were evaluated for intracellular NP-binding and BrdU incorporation. A total of 8×10^6 events were collected per file.

rather infrequent, we did detect NP-binding IgM$^+$ IgD$^-$ CD19$^+$ CD38$^+$ splenic B cells in mice immunized with NP-CγG 57 d previously. Notably, 40–50% of these cells were κ$^+$ (Fig. 7A), and upon exposure to BrdU for 5 d, 25% of NP-binding κ$^+$ cells were BrdU$^+$ (Fig. 7A). Consistent with their designation as memory cells, NP$^+$ IgM$^+$ CD38$^+$ κ$^+$ B cells also exhibited surface expression of CD73 and PDL-2, although CD73$^+$ cells were less frequent among IgM$^+$ cells compared with their IgM$^-$ counterparts (Fig. 7B). Surprisingly, however, we were unable to detect BrdU$^+$ NP-binding κ$^+$ cells in 60-min pulse experiments using the approach described in Fig. 2F, indicating that this population is also not enriched for actively dividing cells. Nonetheless, based on the data in Figs. 4–7, together with the BrdU chase data in Fig. 2B, we conclude that enduring Ab responses to NP-CγG are mediated by a combination

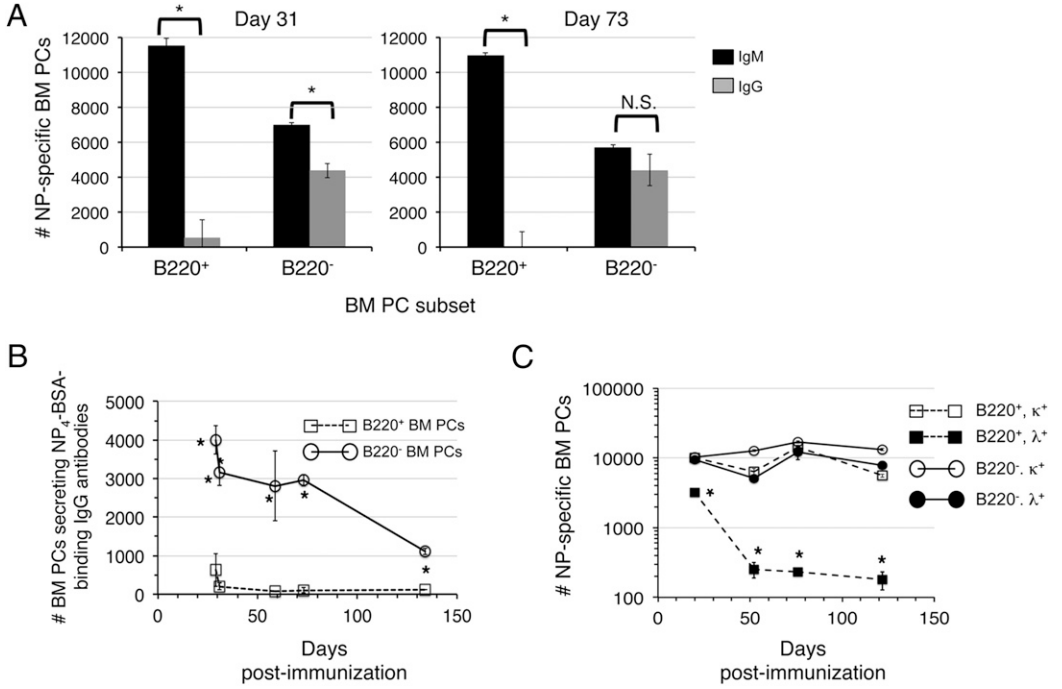

FIGURE 5. Long-term colonization of the BM by IgM-secreting PCs. (**A**) BM PC subsets were sorted and assayed at the indicated time points postimmunization with NP-CγG as described in Fig. 3A using ELISPOT plates coated with NP_{26}-BSA. These plates were probed subsequently with anti–μ-chain or anti–γ-chain Abs. (**B**) Separate experiment wherein sorted BM PC subsets were assayed by ELISPOT at the indicated time points postimmunization using NP_4-BSA–coated plates and anti–γ-chain Abs. (**C**) Additional experiment wherein the indicated BM PC subsets were sorted and assayed for secretion of NP-specific Abs at the indicated time points using NP_{26}-BSA–coated plates and anti-κ or anti-λ Abs. Numbers of hapten-specific PCs in the BM at each time point were calculated as described in *Materials and Methods*. *$p < 0.01$.

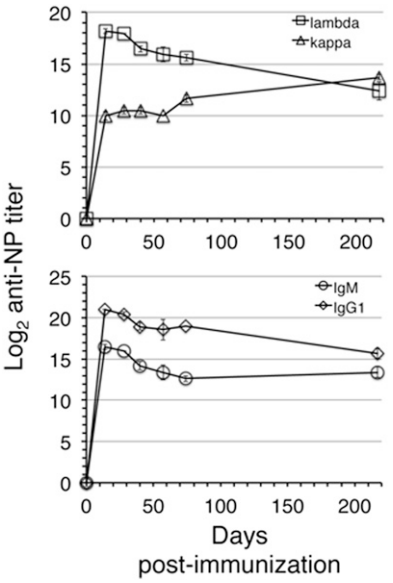

FIGURE 6. Kinetics of serum NP-specific Ab responses. Adult B6 mice were immunized with NP-CγG. On the indicated days postimmunization, serum samples were evaluated for relative titers of NP-specific Igλ- (squares), Igκ- (triangles), IgM- (circles), or IgG1-bearing (diamonds) Abs by ELISA as described in *Materials and Methods*. Data are means and SEMs established from three to four individual mice at each time point.

of long-lived, GC-derived, and recently generated BM PCs, with the latter population derived chiefly from IgM^+ memory B cells.

Discussion

In this work we characterized subpopulations of BM PCs and their roles in long-term humoral responses to a T cell–dependent Ag. Perhaps most notably, we find that ~40% of BM PCs are replaced by recently formed cells every 3–6 d. Thus, although past work introduced the notion that BM PC populations include immature cells (5, 10), we suggest that the BM PC pool is far more dynamic and heterogeneous than expected, with a substantial fraction consisting of recently formed cells. Indeed, based on our BrdU labeling and cell-cycle data, we propose the existence of three subpopulations of BM PCs: short-lived $B220^+$ cells, $B220^-$ cells characterized by an intermediate half-life of 2–3 mo, and a relatively rare population of long-lived $B220^-$ cells. We also find that hapten-specific BM PCs induced by NP-CγG immunization do not consist chiefly of cells secreting high-affinity IgG Abs; rather, our data reveal substantial diversity in IgH usage by BM PCs. In fact, by summing frequencies of IgM- and IgG-secreting PCs across all BM PC subsets, >70 d postimmunization, we estimate that 80% of all NP-specific BM PCs secrete IgM Abs. Together, these findings indicate that PCs derived from several source populations coexist in the BM where they are further characterized by a wide range of half-lives.

The complex nature of the BM PC compartment raises many questions about the factors that regulate its size and the survival of individual cells within long-lived pools. Although many factors may influence PC survival, the extensive heterogeneity among BM PCs raises the possibility that these factors target distinct PC subsets. For instance, PCs often locate adjacent to CXCL12-producing stromal cells in the BM (34). It would be informative to determine whether access to relevant stromal cells and the signals they deliver differs for rapidly versus slowly renewing and/or IgG- versus IgM-secreting BM PCs. Likewise, whereas depletion of cytokines such as BLyS and APRIL or major cell types that secrete these cytokines markedly reduces frequencies of IgG-producing BM PCs (35–37), it is not known whether APRIL also promotes the generation of immature IgM-secreting PCs or

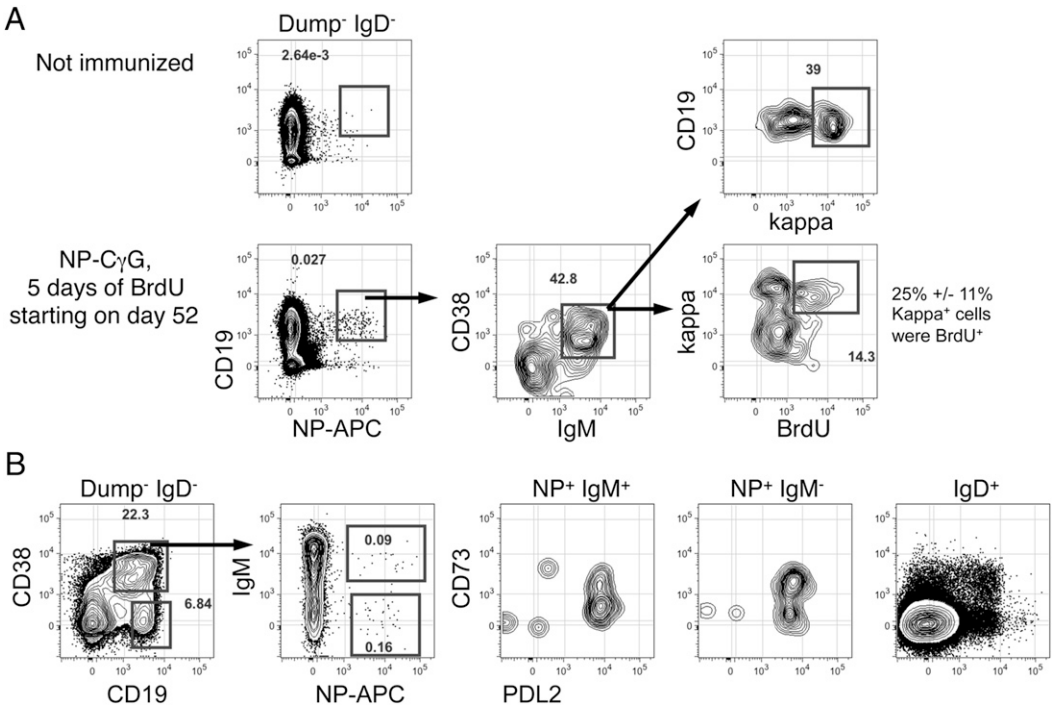

FIGURE 7. Resolution of NP-specific κ^+ IgM^+ memory B cells. (**A**) Adult B6 mice were immunized with NP-CγG. On day 52, mice were given BrdU for 5 d, and on day 57, splenocytes were stained with the indicated reagents to evaluate Igκ surface expression and BrdU incorporation. Numbers in *bottom* of κ versus BrdU plot indicate the mean and SD for the percent $BrdU^+$ cells among NP-binding $IgM\kappa^+$ B cells for five mice. All plots are representative of five mice. (**B**) Separate experiment evaluating CD73 and PDL2 surface expression on IgM^+ and IgM^- NP-binding splenic B cells 60 d postimmunization with NP-CγG. Naive IgD^+ B cells were used as a comparison. Data in (A) and (B) each are representative of two separate experiments. For all samples, we collected 10×10^6 events/file.

their entry into long-lived PC pools. It is tempting to speculate that many immature PCs fail to thrive because of a failure to gain access to APRIL and perhaps other factors. These general considerations apply to cell-intrinsic regulators of PC differentiation and survival as well. One such example concerns the Blimp1 transcription factor encoded by *Prdm1*. Past studies showed that induced deletion of *Prdm1* resulted in a roughly 80% decline in BM PC frequencies (38). Based on our data, we surmise that the decline in BM PC numbers in this study was likely due to the death of preexisting PCs and an arrest in PC differentiation upon induction of Prdm1 deletion. It would be necessary to evaluate the impact of induced Blimp1 deletion on $B220^+$ and $B220^-$ BM PCs to address this and related issues further.

Administration of BrdU in vivo has been an effective tool to identify proliferative cells and to define the steady-state dynamics of cell populations enriched for nonproliferative cells. With this approach, past work has defined steady-state renewal rates for a variety of nonproliferative B-lineage cell population such as immature IgM^+ $IgD^{-/low}$ BM B cells and their immature/transitional counterparts in the adult spleen, where BrdU incorporation occurs mainly within highly mitotic large pre-B cells in the BM. Because of the rapid rate at which immature B cells in the BM and spleen either die or progress into more mature cells, cells in both pools achieve near 100% labeling within 3–4 d (39–41). By contrast, immature PCs in the spleen are thought to consist chiefly of actively dividing PCs or plasmablasts, and also exhibit rapid BrdU labeling rates (20, 22). Therefore, rapid BrdU labeling may be because of active cell division, but may instead reflect rapid cellular turnover of cells within a population enriched for nondividing cells. To address this potentially confusing issue, we evaluated cell division among BM PC subpopulations directly (Fig. 2D–F). Our analyses indicate that, unlike in the spleen, relatively few PCs within the $B220^+$ BM fraction are actively dividing. Therefore, we suggest that the bulk of $B220^+$ BM PCs are immature but nondividing PCs, derived from a proliferative precursor within B memory and/or early PC pools in peripheral lymphoid tissues.

Our inability to detect $BrdU^+$ $B220^-$ PCs in the BM after a 6-d pulse, despite labeling of the bulk of $B220^+$ PCs within this time frame (Fig. 2C), suggests that most $B220^+$ BM PCs fail to gain entry to long-lived niches. Why might so many of these cells fail to mature? As alluded to earlier, additional experiments are needed to establish the capacity of immature BM PCs to use survival factors needed to promote PC longevity and whether the signals they provide are indeed limiting. In this regard, an alternative but not widely considered view is that PC longevity is determined very early during differentiation, irrespective of the environment in which they settle. From this standpoint, PC life span would be determined by limiting signals available only to small numbers of Ag-responsive B cells or newly formed PCs at the inception of PC differentiation. In this scenario, only a small fraction of immature PCs would possess the capacity to receive and translate signals into the transcriptional and epigenetic changes needed for long-term survival. Alternatively, the BM may harbor distinct pools of PCs with unique roles in long-term protection. For instance, $B220^+$ BM PCs may arise from specialized naive B cells in the marginal zone and B1 compartments, because IgM-secreting PCs derived from these pools play unique and important functions in response to bacterial and viral pathogens (42, 43).

Whereas analyses of unimmunized animals revealed the steady-state cellular dynamics of BM PC pools, controlled immunization experiments allowed us to characterize the roles of the BM PC subsets in T cell–dependent humoral immunity. Two aspects of these results were rather unanticipated. First, we originally posited that $B220^+$ BM PCs are a temporary reservoir for GC-derived PCs. However, NP-specific PCs in this pool lacked classic characteristics of GC-derived cells (Fig. 5), and we were able to capture such cells in this population after GC responses evoked by NP-CγG immunization wane (31). Indeed, our data suggest that IgM^+ memory B cells contribute substantially to the BM PC pool long after initiation of Ab responses. These results are consistent with the notion that residual persisting Ag plays important roles in shaping the BM PC pool. However, our results may also reflect chronic stimulation of TLRs on memory B cells as proposed by Lanzavecchia and coworkers (44). Second, despite the dominant role played by $Igλ1^+$ cells in the NP-specific Ab response in B6 mice, at later time points nearly all hapten-specific IgM^+ $B220^+$ BM PCs used Igκ L chains. Past work has shown that NP-specific hybridomas bearing Igκ L chains can be readily derived from B6 mice, provided that such mice are immunized multiple times (45). By contrast, limiting dilution experiments indicate that ∼50% of the naive NP-reactive B cell pool consists of $Igκ^+$-bearing cells (46). Taken together, these results suggest that, although both $Igκ^+$ and $Igλ1^+$ cells become engaged in responses to NP, the latter cells undergo a greater number of cell divisions during early phases of the primary response, and thus are more likely to become engaged with follicular Th cells and form GCs where they eventually yield class-switched cells. By contrast, NP-responsive $Igκ^+$ cells readily generate PCs via a GC-independent pathway (3), but are in general less likely to contribute substantially to classical GC responses.

We were surprised to find that cells secreting NP-specific $IgMκ^+$ Abs can be captured within the $B220^+$ BM PC pool for >100 d postimmunization. We speculate that IgM memory cells possessing stem cell–like properties including limited self-renewal activity contribute to the BM PC pool over extended time frames postimmunization. Stimulation of $CD8^+$ T cells by residual persistent minor alloantigens has been reported to drive the production of memory stem-like cells (47). These cells retain certain characteristics of naive T cells, yet appear to divide slowly while also producing effector T cell populations. Memory IgM^+ B cells may possess similar properties, provided that they are stimulated appropriately by residual Ag or other ligands with the capacity to evoke activation and PC differentiation. Clearly, further work is needed to explore these issues.

Given the multilayered nature of long-term Ab responses to NP-CγG, we are further tempted to speculate about potential advantages of functionally heterogeneous Ab responses. It has been shown that the BCRs expressed by memory B cells possess fewer somatic hypermutation events compared with BM PCs (48). Moreover, many IgM^+ memory cells arise independently of GC-associated maturation pathways (7). Consequently, as proposed by Purtha et al. (49), memory B cells may be readily positioned to respond to alternative epitope structures such as those expressed by viral escape mutants. Therefore, IgM^+ memory cells may play a key role in defending against rapidly evolving viruses by quickly generating short-lived pools of $B220^+$ BM PCs secreting antiviral IgM Abs in a manner analogous to the swiftness with which B cells in the splenic marginal zone generate Abs to blood-borne bacteria (43, 50).

In summary, we found unexpectedly that the BM PC compartment is rather heterogeneous, both with respect to rates of turnover for discrete subpopulations of PCs, and the types of Abs these cells secrete. We suggest that this heterogeneity reflects the multilayered nature of the Ag-responsive peripheral B cell pool, with input from GC B cells and memory B cells derived from this compartment, and B cells with minimal or no participation in GCs such as IgM^+ memory, marginal zone, and perhaps B1 B cells. Understanding the combined roles played by discrete pools of activated and memory

B cells and the PCs they produce in fending off pathogens and in autoimmunity will hopefully lead to improved vaccines and strategies to constrain the activity of pathogenic PCs.

Acknowledgments

We thank Drs. Michael Cancro, Avinash Bhandoola, Michael Carroll, and Stephen Emerson for helpful discussions.

Disclosures

The authors have no financial conflicts of interest.

References

1. Radbruch, A., G. Muehlinghaus, E. O. Luger, A. Inamine, K. G. Smith, T. Dörner, and F. Hiepe. 2006. Competence and competition: the challenge of becoming a long-lived plasma cell. *Nat. Rev. Immunol.* 6: 741–750.
2. Tarlinton, D. M. 2008. Evolution in miniature: selection, survival and distribution of antigen reactive cells in the germinal centre. *Immunol. Cell Biol.* 86: 133–138.
3. Bortnick, A., I. Chernova, W. J. Quinn, III, M. Mugnier, M. P. Cancro, and D. Allman. 2012. Long-lived bone marrow plasma cells are induced early in response to T cell-independent or T cell-dependent antigens. *J. Immunol.* 188: 5389–5396.
4. Foote, J. B., T. I. Mahmoud, A. M. Vale, and J. F. Kearney. 2012. Long-term maintenance of polysaccharide-specific antibodies by IgM-secreting cells. *J. Immunol.* 188: 57–67.
5. Racine, R., M. McLaughlin, D. D. Jones, S. T. Wittmer, K. C. MacNamara, D. L. Woodland, and G. M. Winslow. 2011. IgM production by bone marrow plasmablasts contributes to long-term protection against intracellular bacterial infection. *J. Immunol.* 186: 1011–1021.
6. Taillardet, M., G. Haffar, P. Mondière, M. J. Asensio, H. Gheit, N. Burdin, T. Defrance, and L. Genestier. 2009. The thymus-independent immunity conferred by a pneumococcal polysaccharide is mediated by long-lived plasma cells. *Blood* 114: 4432–4440.
7. Kaji, T., A. Ishige, M. Hikida, J. Taka, A. Hijikata, M. Kubo, T. Nagashima, Y. Takahashi, T. Kurosaki, M. Okada, et al. 2012. Distinct cellular pathways select germline-encoded and somatically mutated antibodies into immunological memory. *J. Exp. Med.* 209: 2079–2097.
8. Taylor, J. J., K. A. Pape, and M. K. Jenkins. 2012. A germinal center-independent pathway generates unswitched memory B cells early in the primary response. *J. Exp. Med.* 209: 597–606.
9. Hauser, A. E., G. F. Debes, S. Arce, G. Cassese, A. Hamann, A. Radbruch, and R. A. Manz. 2002. Chemotactic responsiveness toward ligands for CXCR3 and CXCR4 is regulated on plasma blasts during the time course of a memory immune response. *J. Immunol.* 169: 1277–1282.
10. Kallies, A., J. Hasbold, D. M. Tarlinton, W. Dietrich, L. M. Corcoran, P. D. Hodgkin, and S. L. Nutt. 2004. Plasma cell ontogeny defined by quantitative changes in blimp-1 expression. *J. Exp. Med.* 200: 967–977.
11. Odendahl, M., H. Mei, B. F. Hoyer, A. M. Jacobi, A. Hansen, G. Muehlinghaus, C. Berek, F. Hiepe, R. Manz, A. Radbruch, and T. Dörner. 2005. Generation of migratory antigen-specific plasma blasts and mobilization of resident plasma cells in a secondary immune response. *Blood* 105: 1614–1621.
12. Lindsley, R. C., M. Thomas, B. Srivastava, and D. Allman. 2007. Generation of peripheral B cells occurs via two spatially and temporally distinct pathways. *Blood* 109: 2521–2528.
13. Opstelten, D., and D. G. Osmond. 1983. Pre-B cells in mouse bone marrow: immunofluorescence stathmokinetic studies of the proliferation of cytoplasmic mu-chain-bearing cells in normal mice. *J. Immunol.* 131: 2635–2640.
14. Shaffer, A. L., K. I. Lin, T. C. Kuo, X. Yu, E. M. Hurt, A. Rosenwald, J. M. Giltnane, L. Yang, H. Zhao, K. Calame, and L. M. Staudt. 2002. Blimp-1 orchestrates plasma cell differentiation by extinguishing the mature B cell gene expression program. *Immunity* 17: 51–62.
15. Sanderson, R. D., P. Lalor, and M. Bernfield. 1989. B lymphocytes express and lose syndecan at specific stages of differentiation. *Cell Regul.* 1: 27–35.
16. Kallies, A., E. D. Hawkins, G. T. Belz, D. Metcalf, M. Hommel, L. M. Corcoran, P. D. Hodgkin, and S. L. Nutt. 2006. Transcriptional repressor Blimp-1 is essential for T cell homeostasis and self-tolerance. *Nat. Immunol.* 7: 466–474.
17. Martins, G. A., L. Cimmino, M. Shapiro-Shelef, M. Szabolcs, A. Herron, E. Magnusdottir, and K. Calame. 2006. Transcriptional repressor Blimp-1 regulates T cell homeostasis and function. *Nat. Immunol.* 7: 457–465.
18. Tung, J. W., M. D. Mrazek, Y. Yang, L. A. Herzenberg, and L. A. Herzenberg. 2006. Phenotypically distinct B cell development pathways map to the three B cell lineages in the mouse. *Proc. Natl. Acad. Sci. USA* 103: 6293–6298.
19. O'Connor, B. P., M. Cascalho, and R. J. Noelle. 2002. Short-lived and long-lived bone marrow plasma cells are derived from a novel precursor population. *J. Exp. Med.* 195: 737–745.
20. Ho, F., J. E. Lortan, I. C. MacLennan, and M. Khan. 1986. Distinct short-lived and long-lived antibody-producing cell populations. *Eur. J. Immunol.* 16: 1297–1301.
21. Cancro, M. P., A. P. Sah, S. L. Levy, D. M. Allman, M. R. Schmidt, and R. T. Woodland. 2001. xid mice reveal the interplay of homeostasis and Bruton's tyrosine kinase-mediated selection at multiple stages of B cell development. *Int. Immunol.* 13: 1501–1514.
22. Sze, D. M., K. M. Toellner, C. García de Vinuesa, D. R. Taylor, and I. C. MacLennan. 2000. Intrinsic constraint on plasmablast growth and extrinsic limits of plasma cell survival. *J. Exp. Med.* 192: 813–821.
23. Makela, O., and G. J. Nossal. 1962. Autoradiographic studies on the immune response. II. DNA synthesis amongst single antibody-producing cells. *J. Exp. Med.* 115: 231–244.
24. Wilson, A., E. Laurenti, G. Oser, R. C. van der Wath, W. Blanco-Bose, M. Jaworski, S. Offner, C. F. Dunant, L. Eshkind, E. Bockamp, et al. 2008. Hematopoietic stem cells reversibly switch from dormancy to self-renewal during homeostasis and repair. *Cell* 135: 1118–1129.
25. Srivastava, B., W. J. Quinn, III, K. Hazard, J. Erikson, and D. Allman. 2005. Characterization of marginal zone B cell precursors. *J. Exp. Med.* 202: 1225–1234.
26. Schittek, B., K. Rajewsky, and I. Förster. 1991. Dividing cells in bone marrow and spleen incorporate bromodeoxyuridine with high efficiency. *Eur. J. Immunol.* 21: 235–238.
27. Anderson, S. M., A. Khalil, M. Uduman, U. Hershberg, Y. Louzoun, A. M. Haberman, S. H. Kleinstein, and M. J. Shlomchik. 2009. Taking advantage: high-affinity B cells in the germinal center have lower death rates, but similar rates of division, compared to low-affinity cells. *J. Immunol.* 183: 7314–7325.
28. Pereira, J. P., J. An, Y. Xu, Y. Huang, and J. G. Cyster. 2009. Cannabinoid receptor 2 mediates the retention of immature B cells in bone marrow sinusoids. *Nat. Immunol.* 10: 403–411.
29. Hsu, M. C., K. M. Toellner, C. G. Vinuesa, and I. C. Maclennan. 2006. B cell clones that sustain long-term plasmablast growth in T-independent extrafollicular antibody responses. *Proc. Natl. Acad. Sci. USA* 103: 5905–5910.
30. Takahashi, Y., P. R. Dutta, D. M. Cerasoli, and G. Kelsoe. 1998. In situ studies of the primary immune response to (4-hydroxy-3-nitrophenyl)acetyl. V. Affinity maturation develops in two stages of clonal selection. *J. Exp. Med.* 187: 885–895.
31. Dogan, I., B. Bertocci, V. Vilmont, F. Delbos, J. Mégret, S. Storck, C. A. Reynaud, and J. C. Weill. 2009. Multiple layers of B cell memory with different effector functions. *Nat. Immunol.* 10: 1292–1299.
32. Pape, K. A., J. J. Taylor, R. W. Maul, P. J. Gearhart, and M. K. Jenkins. 2011. Different B cell populations mediate early and late memory during an endogenous immune response. *Science* 331: 1203–1207.
33. Tomayko, M. M., N. C. Steinel, S. M. Anderson, and M. J. Shlomchik. 2010. Cutting edge: hierarchy of maturity of murine memory B cell subsets. *J. Immunol.* 185: 7146–7150.
34. Tokoyoda, K., T. Egawa, T. Sugiyama, B. I. Choi, and T. Nagasawa. 2004. Cellular niches controlling B lymphocyte behavior within bone marrow during development. *Immunity* 20: 707–718.
35. Belnoue, E., C. Tougne, A. F. Rochat, P. H. Lambert, D. D. Pinschewer, and C. A. Siegrist. 2012. Homing and adhesion patterns determine the cellular composition of the bone marrow plasma cell niche. *J. Immunol.* 188: 1283–1291.
36. Benson, M. J., S. R. Dillon, E. Castigli, R. S. Geha, S. Xu, K. P. Lam, and R. J. Noelle. 2008. Cutting edge: the dependence of plasma cells and independence of memory B cells on BAFF and APRIL. *J. Immunol.* 180: 3655–3659.
37. Chu, V. T., A. Fröhlich, G. Steinhauser, T. Scheel, T. Roch, S. Fillatreau, J. J. Lee, M. Löhning, and C. Berek. 2011. Eosinophils are required for the maintenance of plasma cells in the bone marrow. *Nat. Immunol.* 12: 151–159.
38. Shapiro-Shelef, M., K. I. Lin, D. Savitsky, J. Liao, and K. Calame. 2005. Blimp-1 is required for maintenance of long-lived plasma cells in the bone marrow. *J. Exp. Med.* 202: 1471–1476.
39. Allman, D. M., S. E. Ferguson, V. M. Lentz, and M. P. Cancro. 1993. Peripheral B cell maturation. II. Heat-stable antigen(hi) splenic B cells are an immature developmental intermediate in the production of long-lived marrow-derived B cells. *J. Immunol.* 151: 4431–4444.
40. Hartley, S. B., M. P. Cooke, D. A. Fulcher, A. W. Harris, S. Cory, A. Basten, and C. C. Goodnow. 1993. Elimination of self-reactive B lymphocytes proceeds in two stages: arrested development and cell death. *Cell* 72: 325–335.
41. Baumgarth, N., O. C. Herman, G. C. Jager, L. E. Brown, L. A. Herzenberg, and J. Chen. 2000. B-1 and B-2 cell-derived immunoglobulin M antibodies are nonredundant components of the protective response to influenza virus infection. *J. Exp. Med.* 192: 271–280.
42. Martin, F., A. M. Oliver, and J. F. Kearney. 2001. Marginal zone and B1 B cells unite in the early response against T-independent blood-borne particulate antigens. *Immunity* 14: 617–629.
43. Bernasconi, N. L., E. Traggiai, and A. Lanzavecchia. 2002. Maintenance of serological memory by polyclonal activation of human memory B cells. *Science* 298: 2199–2202.
44. Reth, M., G. J. Hämmerling, and K. Rajewsky. 1978. Analysis of the repertoire of anti-NP antibodies in C57BL/6 mice by cell fusion. I. Characterization of antibody families in the primary and hyperimmune response. *Eur. J. Immunol.* 8: 393–400.
45. Stashenko, P., and N. R. Klinman. 1980. Analysis of the primary anti-(4-hydroxy-3-nitrophenyl) acetyl (NP) responsive B cells in BALB/C and B10.D2 mice. *J. Immunol.* 125: 531–537.
46. Zhang, Y., G. Joe, E. Hexner, J. Zhu, and S. G. Emerson. 2005. Host-reactive CD8+ memory stem cells in graft-versus-host disease. *Nat. Med.* 11: 1299–1305.
47. Smith, K. G., A. Light, G. J. Nossal, and D. M. Tarlinton. 1997. The extent of affinity maturation differs between the memory and antibody-forming cell compartments in the primary immune response. *EMBO J.* 16: 2996–3006.
48. Purtha, W. E., T. F. Tedder, S. Johnson, D. Bhattacharya, and M. S. Diamond. 2011. Memory B cells, but not long-lived plasma cells, possess antigen specificities for viral escape mutants. *J. Exp. Med.* 208: 2599–2606.
49. Oliver, A. M., F. Martin, and J. F. Kearney. 1999. IgMhighCD21high lymphocytes enriched in the splenic marginal zone generate effector cells more rapidly than the bulk of follicular B cells. *J. Immunol.* 162: 7198–7207.